02

Selective laser spectroscopy of impurity Ho^{3+} centers in SrY_2O_4 single crystal

© S.I. Nikitin, E.M. Kutashova, R.V. Yusupov, R.G. Batulin, A.G. Kiiamov, I.E. Mumdzhi, B.Z. Malkin

Kazan Federal University,
420008 Kazan, Tatarstan, Russia

e-mail: sergey.nikitin@kpfu.ru

Received November 17, 2022
Revised November 26, 2022
Accepted November 28, 2022

Detailed studies of emission and excitation spectra of impurity Ho^{3+} centers in the SrY_2O_4 single crystal performed by means of the site-selective laser spectroscopy are reported. The energy levels patterns for the $^5I_8$, $^5I_7$, $^5I_6$, $^5S_2$ and $^5F_4$ multiplets of Ho^{3+} ions which substitute for the Y^{3+} ions at the two structurally nonequivalent sites Y1 and Y2 with the local C_s symmetry are constructed by making use of the measured spectra. These energy schemes are well described in the framework of the crystal field theory, the sets of 15 crystal field parameters are determined for Ho^{3+} ions at both Y1 and Y2 sites. The calculated parameters of the EPR spectra agree with the earlier published experimental data.

Keywords: Crystal field, rare-earth ions, site-selective spectroscopy.

DOI: 10.61011/EOS.2023.04.56349.77-22

Introduction

Spectroscopic studies of compounds SrY_2O_4 activated by rare-earth (RE) ions (Sm^{3+}, Eu^{3+}, Dy^{3+}, Tb^{3+}, Er^{3+}) are the subject of a large number of papers. Interest in the study of these compounds is due primarily to the prospects of their use as phosphors for flat displays and light emitting devices. A fairly complete review of research results in this direction is presented in [1]. It should be noted that these studies, as well as studies of other promising phosphors, are devoted to studying the properties of micro- and nanocrystalline powders synthesized by chemical methods, with an emphasis on their light-emitting properties at room and higher temperatures. The spectra given in most papers were measured with a low spectral resolution; analysis of the center composition, the Stark structure of multiplets of RE impurity ions, and the identification of optical transitions are almost impossible.

The second extremely interesting and topical area of research on double oxides of strontium-rare earths is the study of unusual low-temperature magnetic properties of concentrated compounds $SrRE_2O_4$, using the methods of magnetometry and neutron spectroscopy. In particular, the coexistence of magnetic-ordered and disordered subsystems of erbium ($T_N = 0.75\,K$) [2], holmium ($T_N = 0.62\,K$) [3,4], and neodymium ions [5] was discovered. It was shown that there is no long-range magnetic order in $SrDy_2O_4$ crystals upon cooling down to a temperature of 0.02 K [6,7]. An antiferromagnetic noncollinear magnetic structure in the reflection plane of the crystal lattice ($T_N = 0.95\,K$) was found in $SrYb_2O_4$ [8], phase transitions induced by an external magnetic field were observed in $SrHo_2O_4$ [9], $SrDy_2O_4$ [10] and $SrEr_2O_4$ [11]. The variety of registered magnetic structures is due to the quasi-one-dimensional structure of the crystal lattice of orthorhombic symmetry with the space group $Pnam$ ($N62, D_{2h}^{16}$) [12], four magnetically nonequivalent positions of RE ions, competition of single-ion magnetic anisotropy with anisotropic exchange and dipole interactions between RE ions.

The $SrRE_2O_4$ compounds belong to magnets with three-dimensional mixed-type geometric frustrations, the lattice contains beveled ladders (zigzag chains) propagating along the **c** axis, and a honeycomb structure in the **ab** planes (Fig. 1).

The unit cell of the SrY_2O_4 isostructural crystal contains 4 Sr^{2+} ions, 16 O^{2-} ions, and 8 Y^{3+} ions at the 4c Wyckoff positions. Ions Y^{3+} form two subsystems Y1 and Y2, each of which contains 4 crystallographically equivalent sublattices with radius vectors $\mathbf{r}_{1,\lambda} = [ax_\lambda, by_\lambda, 0.25c]$, $\mathbf{r}_{2,\lambda} = [a(0.5-x_\lambda), b(y_\lambda-0.5), 0.75c]$, $\mathbf{r}_{3,\lambda} = -\mathbf{r}_{1,\lambda}$, $\mathbf{r}_{4,\lambda} = -\mathbf{r}_{2,\lambda}$, where a, b and c are crystal lattice constants, $\lambda = Y1, Y2$, x_λ and y_λ are dimensionless structural parameters. The lattice constant $c \sim 0.34\,nm$ is approximately three times smaller than the lattice constants $a \sim 1\,nm$ and $b \sim 1.2\,nm$, each sublattice is formed by chains along the **c** axis. The ions in the magnetically equivalent chains located in positions with the basis vectors $\mathbf{r}_{1,\lambda}$ and $\mathbf{r}_{3,\lambda}$ ($\mathbf{r}_{2,\lambda}$ and $\mathbf{r}_{4,\lambda}$) form ladders along the **c** axis and are shifted relative to each other by $c/2$. These ladders can be considered as zigzag chains with slightly different distances between the first ($\sim 0.35\,nm$ and $\sim 0.355\,nm$ in Y1 and Y2 ion chains, respectively) and the second (lattice constant c in all the chains) neighbors. The crystal structure contains two types of ladders (positions $\mathbf{r}_{1,\lambda}$, $\mathbf{r}_{3,\lambda}$ and $\mathbf{r}_{2,\lambda}$, $\mathbf{r}_{4\lambda}$), their planes are rotated around the c axis relative to each other by an angle $\sim \pi/3$. The Y^{3+} ions are

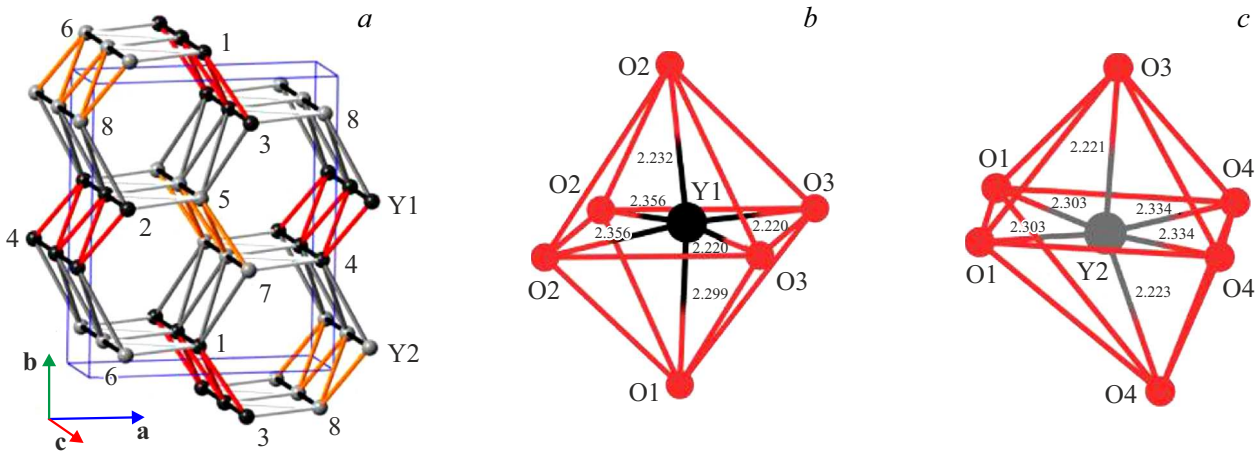

Figure 1. Fragments of the SrY_2O_4 crystal structure: (a) Y1 and Y2 sublattices, (b, c) and the nearest oxygen environment of yttrium ions.

located in distorted oxygen octahedra, the point symmetry group is C_s for both positions Y1 and Y2 (Fig. 1, *b, c*). RE ions in positions with basis vectors $\mathbf{r}_{1,\lambda}$ and $\mathbf{r}_{3,\lambda}$ ($\mathbf{r}_{2,\lambda}$ and $\mathbf{r}_{4,\lambda}$) are magnetically equivalent.

The first step in constructing a microscopic model of the magnetic properties of a rare earth compound is to determine the excitation spectrum of the electronic subsystem and the symmetry of the wave functions of the sublevels of the ground multiplet of the rare earth ion in a crystal field (CF). To solve this problem in the case of a multicenter system of holmium ions in an $SrHo_2O_4$ crystal, we studied the spectral characteristics of isostructural diamagnetic SrY_2O_4 crystals with low concentrations of impurity Ho^{3+} ions replacing Y^{3+} ions by optical selective laser spectroscopy.

It should be noted that earlier estimates of the energies of a number of electronic excitations in the $SrHo_2O_4$ crystal were obtained by measuring the spectra of inelastic neutron scattering [13,14]. The submillimeter EPR spectra of Ho^{3+} impurity ions in SrY_2O_4 single crystals were measured in [15].

Samples and measurement procedure

Single-crystals of SrY_2O_4, doped with Ho^{3+} ions, were grown by the optical floating zone technique similarly [16]. The application of this method is due to the high melting temperature (2170°C) of SrY_2O_4 crystals. $SrCO_3$ (Alfa Aesar, 99.99%), Y_2O_3 (Alfa Aesar, 99.99%) and Ho_2O_3 (Alfa Aesar, 99.9%) were used as starting materials, the concentration of Ho^{3+} ions in the initial charge was 0.2 at.%. Solid-phase synthesis was carried out at the first step. Carefully milled stoichiometric composition was annealed at a temperature of 1050°C for 8 h. The result of the synthesis was controlled by X-ray diffraction analysis on a Bruker D8 ADVANCE diffractometer. The measurement results showed that the synthesized powder is single-phase, the lattice constants and the space symmetry group correspond to the compound SrY_2O_4. From the powder obtained, a cylindrical billet 5 mm in diameter and 70 mm long was formed under a hydrostatic pressure. Crystal growth was carried out in an air flow (air flow rate 0.5 l/min) on an FZT-4000-H-VII-VPO-PC optical floating zone unit (Crystal Systems Corp., Japan). The pulling speed through the melting zone was 3 mm/h. To ensure the homogeneity of the melting zone, the lower and upper parts of the grown crystal (relative to the melt zone) rotated in opposite directions at a 15 rot/min speed.

The grown crystals were transparent and colorless. X-ray diffraction analysis showed that the crystals are also single-phase, and their structure corresponds to the compound SrY_2O_4. The lattice constants $a = 1.007437$ nm, $b = 1.19116$ nm, $c = 0.3407$ nm and the coordinates of atoms in the lattice cell are determined at room temperature, in particular, $x_{Y1} = 0.42312$, $y_{Y1} = 0.11043$, $x_{Y2} = 0.42346$, $y_{Y2} = 0.61229$, $x_{O1} = 0.21379$, $y_{O1} = 0.17172$, $x_{O2} = 0.12494$, $y_{O2} = 0.47966$, $x_{O3} = 0.51025$, $y_{O3} = 0.78370$, $x_{O4} = 0.42429$, $y_{O4} = 0.42568$. Samples for research were cut from grown crystals in the shape of a parallelepiped and had dimensions $3 \times 3 \times 4$ mm. To carry out optical measurements, the samples were not oriented relative to the crystallographic axes; the faces of the parallelepiped were polished.

For measurements by selective laser spectroscopy, a pulsed laser based on a Coumarin-153 dye solution was used as a luminescence excitation source; the emission linewidth was 0.4 Å. Pumping was carried out by the third harmonic of a YAG:Nd laser (LQ129, Solar LS). The wavelength and linewidth of laser radiation were determined by a wide-range wavelength meter (SHR, Solar LS). The luminescence registration system used an MDR-23 monochromator, cooled FEU-106 photomultipliers (thermoelectric cooling) and FEU-83 (cooling with liquid nitrogen vapor), operating in the photon counting mode. The luminescence kinetics was measured using a Turbo

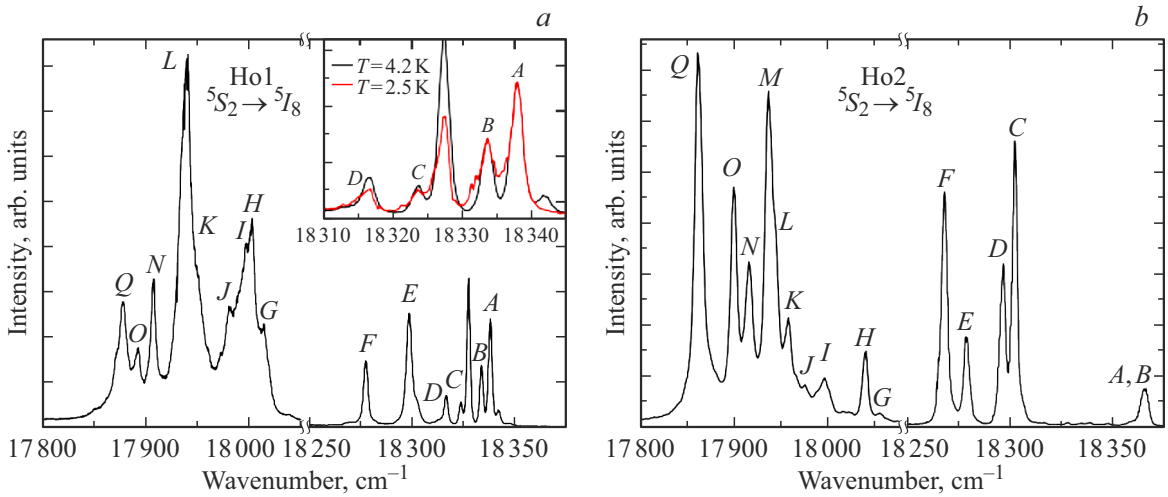

Figure 2. Selectively excited luminescence spectra of impurity Ho^{3+} ions ($^5S_2 \rightarrow {}^5I_8$) in SrY_2O_4:Ho (0.2 at.%) crystal, $T = 4.2$ K. (*a*) Excitation energy $\nu_{exc} = 18572.7\,cm^{-1}$, luminescence corresponds to transitions from the sublevels of the lowest quasi-doublet (Γ_1, Γ_2, — 18337.9 and 18341.7 cm^{-1}) of the $^5S_2$ multiplet of Ho1 ions. The inset shows the transformation of the short-wavelength part of the luminescence spectrum as the temperature is lowered to 2.5 K. (*b*) The excitation energy is 18644.7 cm^{-1}; emission corresponds to transitions from the lower quasi-doublet (Γ_1, Γ_2, 18365.5 cm^{-1}) of the $^5S_2$ multiplet of Ho2 ions.

MCS multichannel scalar. The sample under study was placed in a helium-filled cryostat and was in helium vapor at a temperature of 4.2 K; in a number of experiments, the sample temperature was lowered to approximately 2.5 K by pumping out helium vapor.

Experimental findings

According to X-ray diffraction data, upon activation of SrY_2O_4 crystals by RE ions, minimum two types of structurally nonequivalent impurity centers can be formed corresponding to the substitution of RE ions for Y^{3+} ions. Luminescence excitation was carried out in multiplets $^5S_2$, $^5F_4$. The luminescence of the sample under study was registered in a wide spectral range and corresponded to the following transitions ions Ho^{3+}: $^5S_2 \rightarrow {}^5I_8$, $^5S_2 \rightarrow {}^5I_7$, $^5S_2 \rightarrow {}^5I_6$, $^5F_5 \rightarrow {}^5I_8$, $^5I_5 \rightarrow {}^5I_8$, $^5I_6 \rightarrow {}^5I_8$. The most intense luminescence corresponded to transitions from the $^5S_2$ multiplet. By selecting the excitation wavelength, it was possible to isolate two sets of levels of predominant centers of Ho^{3+} ions with different structures in the observed luminescence spectra. It should be noted that other luminescence spectra of Ho^{3+} ions were observed as well, but their luminescence intensity was more than two orders of magnitude lower. Fig. 2 shows the luminescence spectra of two impurity centers of Ho^{3+} ions. Based on the totality of experimental data presented in this paper, and data obtained by the EPR method, an unambiguous theoretical interpretation of the observed luminescence and luminescence excitation spectra was achieved. For this reason, in this figure and further in the paper, the designations of the centers Ho1 and Ho2 are introduced, corresponding to the impurity centers of Ho^{3+} ions in positions Y1 and Y2, respectively. In Fig. 2, the letters denote the Stark sublevels of the multiplet $^5I_8$, corresponding to the designations given in Table 1. Similar designations are presented in other figures.

In the luminescence spectrum of the Ho1 center shown in Fig. 2, a structure of spectral lines is observed due to the splitting of the $^5S_2$ multiplet, the splitting of the lower quasi-doublet is 3.8 cm^{-1}. This conclusion is confirmed by the transformation of the luminescence spectrum with decreasing temperature to 2.5 K — the intensities of the lines corresponding to transitions from the upper sublevel of the quasi-doublet decrease (see insert in Fig. 2, *a*). The energy gap between the *A* and *B* lines (4.3 cm^{-1}) corresponds to the distance between the lower stark sublevels of the $^5I_8$ multiplet. In the luminescence spectrum of the Ho2 center, the resonance line (*A*, *B* 18 365 cm^{-1}) corresponding to the transitions between the lowest stark sublevels of the $^5I_8$ and $^5S_2$ multiplets is approximately 2 times wider compared to adjacent lower-energy lines (*C*, *D*, *E* and *F*, Fig. 2, *b*), there is no additional structure. This indicates a small splitting of the ground quasi-doublet of the $^5I_8$ multiplet; there is no splitting of the lower stark sublevel of the $^5S_2$ multiplet in the luminescence spectrum.

The luminescence kinetics of Ho1 and Ho2 impurity centers, corresponding to transitions between the $^5S_2$ and $^5I_8$ multiplets, is shown in Fig. 3. The luminescence kinetics is single-exponential for both centers, there is no transfer of electronic excitation energy between the Ho^{3+} ions. This fact allows to successfully apply the method of selective laser excitation for separating the luminescence spectra of structurally nonequivalent impurity centers of Ho^{3+}. The luminescence lifetimes of Ho1 and Ho2 ions from the $^5S_2$ multiplet are $225 \pm 1\,\mu s$ and $257 \pm 1\,\mu s$, respectively.

Table 1. Measured and calculated energies (cm^{-1}) of the Stark sublevels of impurity Ho^{3+} ion multiplets in SrY_2O_4

$^{2S+1}L_J$		Ho1			Ho2		
		Γ	Experiment	Theory	Γ	Experiment	Theory
$^5I_8$	*A*	2	0	0	1	0	0
	B	2	4.3	4.35	2	< 2.5	1.64
	C	1	14.7	14.3	2	62.1	62.9
	D	1	25.6	24.7	2	67.7	67.7
	E	2	39.5	38.4	1	85.3	86.5
	F	1	61.3	59.4	1	95.8	97.7
	G	2	324	325.8	2	311	315.8
	H	1	335.6	331.5	1	327	317.7
	I	2	341	347.0	2	369.5	369.4
	J	1	357	378.7	2	389.8	384.2
	K	2	389	381.7	1	407.4	408.4
	L	1	398.8	390	2	–	418.2
	M	1	423.8	420.6	1	429.5	418.5
	N	2	431	431.8	1	449.9	442.4
	O	2	445.7	443.2	1	466.3	463.1
	P	1	–	446.2	2	–	487.5
	Q	1	460.3	457.8	1	504	490.2
$^5I_7$	*A*	2	5167.4	5165.3	2	5143.4	5142.9
	B	2	–	5166.0	1	–	5143
	C	1	5172.4	5169.9	2	5219.1	5220.3
	D	2	5176.9	5176.1	1	5224.4	5223
	E	1	5179.8	5177.5	2	–	5225.5
	F	1	5185.4	5183.7	1	5231.3	5230
	G	2	5319.9	5314.9	2	5312.4	5308.8
	H	2	5333.5	5330.5	1	–	5315.8
	I	1	–	5337.1	2	5369.2	5368.4
	J	1	5355.5	5352.5	1	–	5371.4
	K	2	5357.3	5355.8	1	5387.5	5389.1
	L	1	5380.3	5368.1	2	5400.2	5392.9
	M	2	5415.1	5408.6	2	5421.6	5421.4
	N	2	5444.6	5429.7	1	–	5461.3
	O	1	5446.7	5430.7	2	5483.5	5465.5
$^5I_6$	*A*	1	8678.2	8679.9	2	8662	8661.6
	B	2	8681.2	8682.8	1	8664.3	8663.1
	C	1	8685.7	8683.2	1	8721.2	8722.6
	D	1	8699	8694.9	2	8727.7	8729
	E	2	8705.4	8703.6	1	8744.5	8743.4
	F	2	8751.7	8759.5	2	8782.4	8790.1
	G	1	8787.9	8799.7	1	8797.6	8802.7
	H	1	8791.2	8804.8	2	8832.7	8823.4
	I	2	8796.7	8808.8	1	8849.7	8845.6
	J	1	8822.5	8825.4	2	8854.6	8852.2
	K	2	8844.1	8849.2	1	–	8866.3
	L	2	8904.6	8895.3	2	8950.3	8932.8
	M	1	8914.2	8912.8	1	8956.1	8941.6
$^5S_2$	*A*	1	18337.9	18339	1	18365.5	18364
	B	2	18341.7	18341	2	–	18366
	C	2	–	18371	2	18414.8	18413
	D	1	18373.3	18375	1	–	18413
	E	1	18384.9	18381	1	18418.8	18417

Table 1. *Continued*

$^{2S+1}L_J$		Ho1			Ho2		
		Γ	Experiment	Theory	Γ	Experiment	Theory
$^5F_4$	*a*	2	18453.1	18454	1	18479.7	18493
	b	1	18481.7	18479	2	–	18496
	c	1	–	18512	2	18536.4	18539
	d	2	18524.9	18529	1	18547.9	18551
	e	2	18534.7	18535	1	18560.1	18569
	f	1	18538.7	18557	2	18595.3	18599
	g	2	18572.7	18564	1	18613.1	18600
	h	1	18580.1	18573	2	18634.3	18627
	i	1	18598.5	18581	1	18647.7	18647

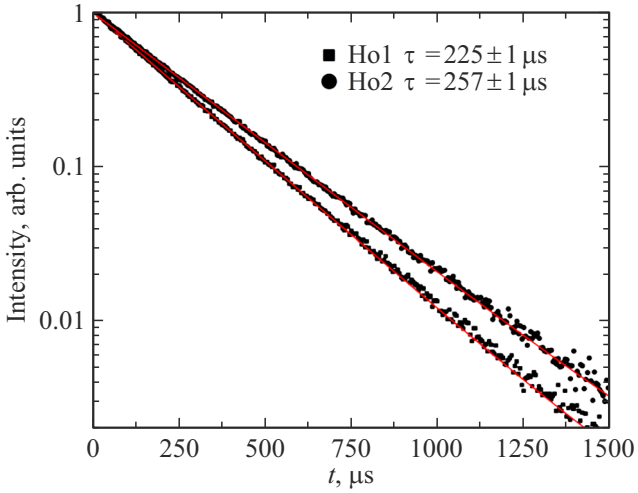

Figure 3. Kinetics of $^5S_2 \rightarrow {}^5I_8$ luminescence Ho1 centers (■ — excitation of luminescence $\nu_{exc} = 18572.7\,cm^{-1}$, registration of luminescence $\nu_{reg} = 18014\,cm^{-1}$) and Ho2 (● — $\nu_{exc} = 18634.3\,cm^{-1}$, $\nu_{reg} = 17862.4\,cm^{-1}$), $T = 4.2$ K.

These lifetime values were used to check the assigment of lines in the luminescence spectra from the $^5S_2$ multiplet to the Ho1 and Ho2 ion centers.

The luminescence excitation spectra from the $^5S_2$ multiplet were measured by recording the luminescence corresponding to transitions between the $^5S_2$ and $^5I_6$ multiplets (Fig. 4). In this case, the excitation and detection wavelengths are very different (luminescence detection is at $\nu_{reg} = 9632.5\,cm^{-1}$ for Ho1, luminescence detection is at $\nu_{reg} = 9510.4\,cm^{-1}$for Ho2), which allowed to measure the nonoverlapping excitation spectra of both impurity Ho^{3+} ion centers. In Fig. 4, the designations of the lines correspond to the data given in Table 1.

The excitation spectrum of the Ho1 center shows lines corresponding to transitions from both the ground and the first excited Stark sublevels of the $^5I_8$ multiplet. To isolate the lines corresponding to transitions from the first excited sublevel, the energy of which is $4.3\,cm^{-1}$, we measured the corresponding luminescence excitation spectrum at 2.5 K. The lines in Fig. 4, *a*, which are marked with letters

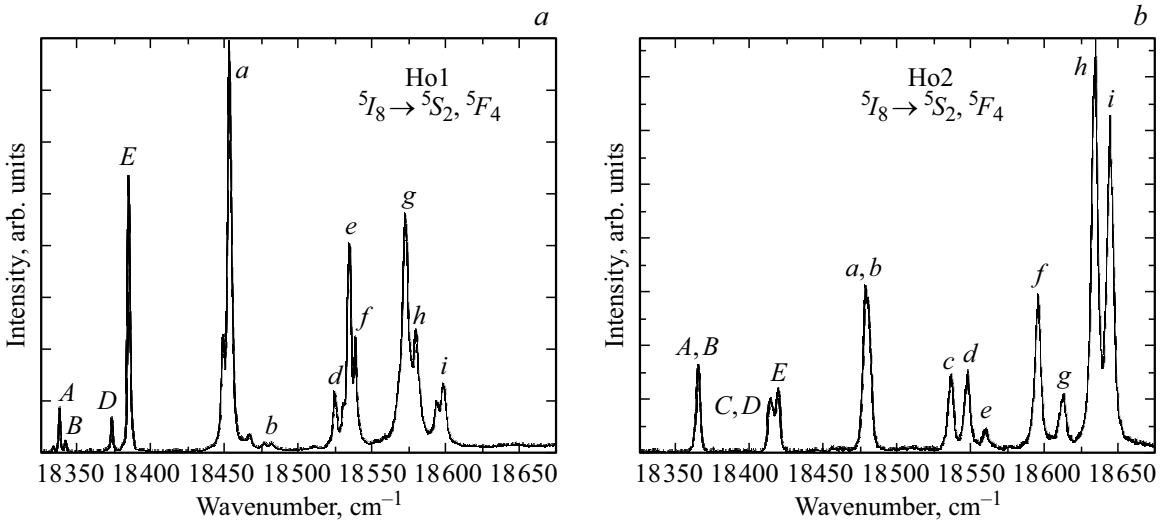

Figure 4. Luminescence excitation spectra corresponding to luminescence from the $^5S_2$ multiplet of the crystal $SrY_2O_4:Ho^{3+}$ (0.2 at.%), $T = 4.2$ K: (*a*) luminescence at $\nu_{reg} = 9632.5\,cm^{-1}$, (*b*) excitation spectrum of Ho2 ions detected at $\nu_{reg} = 9510.4\,cm^{-1}$.

according to Table 1, correspond to transitions from the ground Stark sublevel of the multiplet $^5I_8$.

In contrast to the luminescence excitation spectrum of Ho1 ions, all lines have a much wider width in the excitation spectrum of Ho2 ions. Thus, the resonance line in the spectrum of Ho2 ions has a width of approximately 4.5 cm^{-1}, which is three times greater than the width of the resonance line in the excitation spectrum of Ho1 ions. Let us note that the widths of the resonance line in the luminescence spectra (Fig. 2, *b*) and luminescence excitation practically coincide. This fact can only be explained by the presence of a splitting smaller than the linewidth ($< 2.5\,cm^{-1}$) of the ground quasi-doublet of the $^5I_8$ multiplet. The line at frequency $\nu = 18\,479.7\,cm^{-1}$ (line *a, b*, Fig. 4, *b*) has a width of approximately 5.8 cm^{-1}, which is almost 1.5 times greater linewidth with frequency $\nu = 18\,536.4\,cm^{-1}$ (linewidth $\approx 4\,cm^{-1}$), which corresponds to the transition to the Stark sublevel of the multiplet $^5F_4$ with higher energy. Thus, it can be assumed that the linewidth *a, b* is due to transitions to the Stark sublevels of the multiplet $^5F_4$, the energy gap between which is smaller than the observed linewidth. The assumptions about the structure of $^5S_2$, $^5F_4$ and $^5I_8$ multiplets made as part of the analysis of the luminescence excitation spectrum of Ho2 ions agreed very well with the calculations, the details of which are discussed in the next section (Table 1).

Fig. 5 shows the luminescence spectra of Ho1 and Ho2 ions corresponding to the $^5S_2 \rightarrow {}^5I_7$ transitions. In the luminescence spectrum of the center Ho1 (Fig. 5, *a*), as well as in the luminescence spectrum corresponding to transitions to the sublevels of the $^5I_8$ multiplet (Fig. 2, *a*), there are lines due to transitions from the upper sublevel of a quasi-doublet with an energy of 18 341.7 cm^{-1}. The intensity of these lines decreased in the luminescence spectrum measured at a temperature of 2.5 K. The lines corresponding to transitions from the lower sublevel of the quasi-doublet with an energy of 18 337.9 cm^{-1} are denoted in Fig. 5, *a* by letters according to Table 1.

In the luminescence spectrum ($^5S_2 \rightarrow {}^5I_7$) of impurity centers of Ho2 ions (Fig. 5, *b*), the resonance line at a frequency of 13 221.6 cm^{-1} (line *A, B* in the figure) has a width of $\approx 3.6\,cm^{-1}$, which is 1.5 times larger than the widths of closely spaced lines (*C*, *D* and *F*). It can be concluded that this line corresponds to transitions to the split lower quasi-doublet of the multiplet $^5I_7$ (the splitting of which is less than 1 cm^{-1}). The lines with energies 13 170.6 and 13 158.2 cm^{-1} observed from the short-wavelength side of the *C* line are due to the luminescence of additional ion centers Ho^{3+}, the concentration of which is low (the intensity of the observed lines is approximately 30 times less than the intensity of the line *C*), with optical transition energies that differ significantly from the transition energies in the Ho1 and Ho2 centers. The luminescence kinetics during registration on the lines 13 170.6 and 13 158.2 cm^{-1} are single-exponential, the lifetimes are almost the same and equal to 243 ± 1 and $239 \pm 1\,\mu$s, respectively, and differ markedly from the lifetime of luminescence from the $^5S_2$ multiplet of Ho1 and Ho2 centers (225 ± 1 and $257 \pm 1\,\mu$s respectively). The luminescence excitation spectra also differ markedly from the excitation spectra of Ho1 and Ho2 ions during registration on these lines. Thus, the lines with energies 13 170.6 and 13 158.2 cm $^{-1}$ refer to two different centers of Ho^{3+} ions , the concentration of which is much lower than the concentration of Ho1 and Ho2 centers. Due to the overlap of the luminescence excitation spectra of these centers with the excitation spectrum of Ho2 ions, it was not possible to select the conditions for excitation of luminescence under which lines with the same frequency would not be observed in the luminescence spectrum of

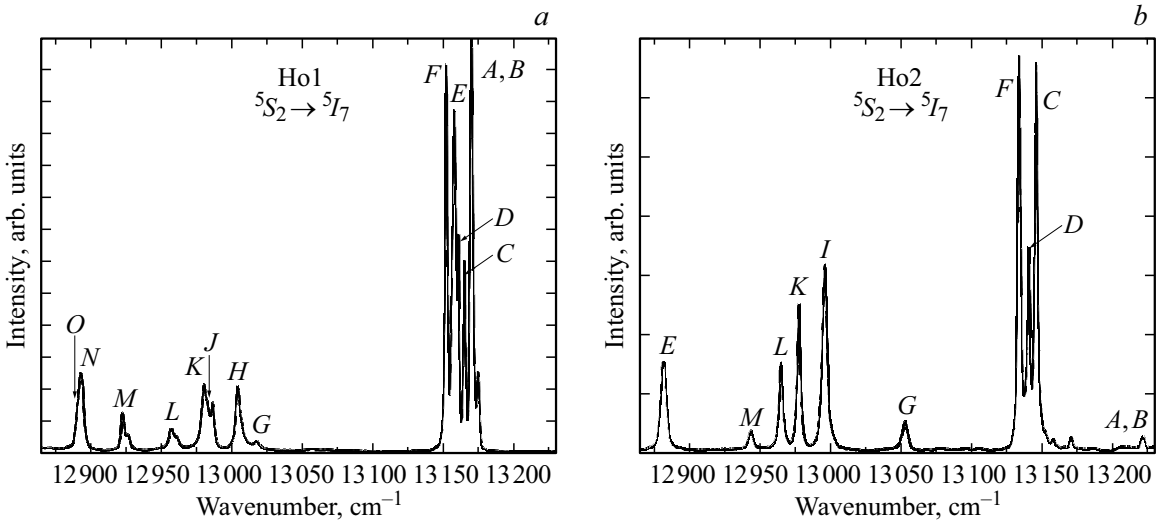

Figure 5. Luminescence spectra of impurity ions Ho^{3+} ($^5S_2 \rightarrow {}^5I_7$) in an SrY_2O_4:Ho (0.2 at.% crystal), $T = 4.2$ K (*a*) Excitation energy $\nu_{exc} = 18453.1\,cm^{-1}$, luminescence corresponds to transitions from the sublevels of the lowest quasi-doublet (Γ_1, Γ_2 — 18337.9 and 18341.7 cm^{-1}) of the $^5S_2$ multiplet of Ho1 ions; (*b*) excitation energy 18634.3 cm^{-1}, radiation corresponds to transitions from the lowest quasi-doublet (Γ_1, Γ_2, 18365.5 cm^{-1}) of the $^5S_2$ multiplet of Ho2 ions.

$^5S_2 \rightarrow {}^5I_7$ of Ho2 ions. In Fig. 5, *b* the luminescence lines of Ho2 ions are marked according to Table 1.

Upon excitation of luminescence from the $^5S_2$ and $^5F_4$ multiplets of both Ho1 and Ho2 centers, there were low-intensity luminescence spectra corresponding to the $^5I_5 \rightarrow {}^5I_8$, $^5I_6 \rightarrow {}^5I_8$ and $^5F_5 \rightarrow {}^5I_8$ transitions. The set of experimental data on the energies of the Stark sublevels of the $^5I_8$ multiplet of the Ho1 and Ho2 centers, obtained from the analysis of the luminescence spectra data, fully corresponds to the energies of the Stark sublevels of the $^5I_8$ multiplet given in Table 1.

Simulation of measured spectra and discussion of results

The analysis of the Stark structure of the Ho^{3+} ion spectra constructed on the basis of the performed measurements was carried out using the Hamiltonian determined in the total space of 1001 states of the ground electronic configuration $4f^{10}$,

$$H = H_{F1} + H_{CF}, \tag{1}$$

where the operator

$$H_{F1} = \xi \sum_k \hat{\mathbf{l}}_k \hat{\mathbf{s}}_k + \alpha \hat{\mathbf{L}}^2 + \beta \hat{G}(G_2) + \gamma \hat{G}(R_7) + \sum_q (F^q \hat{f}_q + P^q \hat{p}_q + T^q \hat{t}_q + M^q \hat{m}_q) \tag{2}$$

is the Hamiltonian of a free ion written in standard form [17], which contains the energies of the spin-orbit interaction ($\mathbf{l}_k$ and $\mathbf{s}_k$ are orbital and spin moments of $4f$ electrons, respectively), electrostatic interactions between $4f$ electrons (numbered by index k) and additional terms corresponding to relativistic interactions and mixing of the ground and excited electronic configurations, $\mathbf{L}$ is the total orbital momentum of electrons. $\hat{G}$, $\hat{f}$, $\hat{p}$, $\hat{t}$, $\hat{m}$ operators are given in the literature [17]. In the calculations of the spectra, the initial values of the parameters of the operator (2) from [18] were used, they were corrected on the basis of the measured energies of the centers of gravity of the multiplets; the parameters obtained as a result of variation are (in cm^{-1})

$$F_2 = 93128 \pm 50,\ F_4 = 66972 \pm 25,\ F_6 = 51860,$$
$$\xi = 2132,\ \alpha = 18.9,\ \beta = -618,\ \gamma = 1840 \pm 15,$$
$$P_2 = 605,\ P_4 = 302.5,\ P_6 = 210.5,$$
$$M_0 = 2.79,\ M_2 = 0.56\,M_0,\ M_4 = 0.38\,M_0,$$
$$T_2 = 400,\ T_3 = 37,\ T_4 = 107,\ T_6 = -264,$$
$$T_7 = 316,\ T_8 = 354 \pm 18.$$

When modeling the spectra, different values of the F_2, F_4, γ and T_8 parameters were obtained, the upper and lower signs in the $\pm$ symbol determine the parameters of holmium ions in positions Y1 and Y2, respectively.

The operator H_{CF} determines the energy of localized $4f$ electrons in the static CF of the C_s symmetry in the Cartesian coordinate system with the axes x, y, z along the crystallographic axes **a**, **b**, **c**, respectively:

$$H_{CF} = B_2^0 O_2^0 + B_2^2 O_2^2 + B_2^{-2} O_2^{-2} + B_4^0 O_4^0 + B_4^2 O_4^2 + B_4^{-2} O_4^{-2} + B_4^4 O_4^4 + B_4^{-4} O_4^{-4} + B_6^0 O_6^0 + B_6^2 O_6^2 + B_6^{-2} O_6^{-2} + B_6^4 O_6^4 + B_6^{-4} O_6^{-4} + B_6^6 O_6^6 + B_6^{-6} O_6^{-6}. \tag{3}$$

Here operators O_p^q are linear combinations of components of spherical tensor operators $C_q^{(p)}$ and $C_{-q}^{(p)}$ [19], B_p^q are CF parameters. The spectra were calculated using two independent sets of CF parameters for holmium ions Ho1 and Ho2 in structurally nonequivalent positions Y1 (sublattices with basis vectors $\mathbf{r}_{m,\mathrm{Y1}}$, $m = 1, 2, 3, 4$) and Y2 (sublattices $\mathbf{r}_{m,\mathrm{Y2}}$). B_p^q CF parameters for Ho1 (Ho2) ions in the $\mathbf{r}_{m,\mathrm{Y1}}$ ($\mathbf{r}_{m,\mathrm{Y2}}$) sublattices have the same absolute values, but the parameters B_p^{-q} ($q > 0$) for ions in the $\mathbf{r}_{1,\lambda}$, $\mathbf{r}_{3,\lambda}$ and $\mathbf{r}_{2,\lambda}$, $\mathbf{r}_{4,\lambda}$ sublattices have opposite signs. The initial values of the CF parameters were calculated in framework of the exchange charge model [16,20] and then varied in order to describe the measured Stark structure of the multiplets and EPR spectra presented earlier in [15]. When modeling the EPR spectra, the Hamilton (1) was supplemented by the interaction operators of the holmium ion with an external magnetic field B (H_z), and magnetic dipole (H_{HFM}) and electric quadrupole (H_{HFQ}) hyperfine interaction operators:

$$H_Z = \mu_{\mathrm{B}} \sum_j (\mathbf{l}_j + 2\mathbf{s}_j)\mathbf{B} - \gamma_{\mathrm{Ho}}\hbar \mathbf{I}\mathbf{B}, \tag{4}$$

$$\begin{aligned} H_{\mathrm{HFM}} = 2\mu_{\mathrm{B}}\gamma_{\mathrm{Ho}}\hbar \left\langle \frac{1}{r^3} \right\rangle_{4f} \sum_k \Bigg\{ \mathbf{I}\mathbf{l}_k + \frac{\sqrt{6}}{2} \Bigg[\frac{2}{\sqrt{6}} C_{0,k}^{(2)} \\ \times (3 s_{kz} I_z - \mathbf{s}_k \mathbf{I}) + (C_{2,k}^{(2)} + C_{-2,k}^{(2)})(s_{kx} I_x - s_{ky} I_y) \\ - i(C_{2,k}^{(2)} - C_{-2,k}^{(2)})(s_{kx} I_y + s_{ky} I_x) \\ - (C_{1,k}^{(2)} - C_{-1,k}^{(2)})(s_{kx} I_z + s_{kz} I_x) \\ + i(C_{1,k}^{(2)} + C_{-1,k}^{(2)})(s_{kz} I_y + s_{ky} I_z) \Bigg] \Bigg\}, \end{aligned} \tag{5}$$

$$\begin{aligned} H_{\mathrm{HFQ}} = \frac{e^2 Q(1-\gamma_\infty)}{4I(2I-1)} \sum_L \frac{q_L}{r_L^5} \Big[(3z_L^2 - r_L^2) I_0 + 3(x_L^2 - y_L^2) I_2 \\ + 6 x_L y_L I_{-2} \Big] - \frac{\sqrt{6} e^2 Q(1-R_Q)}{4I(2I-1)} \left\langle \frac{1}{r^3} \right\rangle_{4f} \\ \times \sum_k \Bigg[\frac{\sqrt{6}}{3} C_{0,k}^{(2)} I_0 + (C_{2,k}^{(2)} + C_{-2,k}^{(2)}) I_2 \\ - i(C_{2,k}^{(2)} - C_{-2,k}^{(2)}) I_{-2} - (C_{1,k}^{(2)} - C_{-1,k}^{(2)}) I_1 \\ + i(C_{1,k}^{(2)} + C_{-1,k}^{(2)}) I_{-1} \Bigg]. \end{aligned} \tag{6}$$

In formulas (4)–(6) μ_{B} is the Bohr magneton, e is the proton charge, $\mathbf{r}$ is the radius vector of $4f$-electron, $\langle r^{-3} \rangle_{4f} = 9.7$ at.units [21], $I = 7/2$ is the holmium nucleus spin, $\gamma_{\mathrm{Ho}}/2\pi = 8.98$ MHz/T is the nuclear gyromagnetic ratio and $Q = 2.394 \cdot 10^{-28}$ m^2 is the nuclear quadrupole moment of ^{165}Ho, $\gamma_\infty = -80$ and $R_Q = 0.1$ – are the antishielding and Sternheimer shielding factors, respectively [22], $I_0 = 3I_z^2 - I(I+1)$, $I_1 = I_x I_z + I_z I_x$, $I_{-1} = I_z I_y + I_y I_z$, $I_2 = I_x^2 - I_y^2$, $I_{-2} = I_x I_y + I_y I_x$. The upper line in (6) determines the interaction energy of the quadrupole moment of the nucleus with the electric field gradient of the ionic lattice, the summation is carried out by the Ewald method over lattice ions with nominal charges eq_L ($q_{\mathrm{Sr}} = 2$, $q_{\mathrm{Y}} = 3$, $q_{\mathrm{O}} = -2$) and radius vectors $\mathbf{r}_L$ relative to the position of the holmium ion under consideration. The calculated lattice sums are (in units of nm^{-3}):

$$\sum_L q_L (3z_L^2 - r_L^2)/r_L^5 = -14.4 \text{ and } 36.4,$$

$$\sum_L q_L (x_L^2 - y_L^2)/r_L^5 = -7.32 \text{ and } 74.0,$$

$$\sum_L q_L x_L y_L / r_L^5 = 1.24 \text{ and } -1.55$$

for Ho1 and Ho2 ions, respectively. In the cubic CF of a regular oxygen octahedron, the ground multiplet $^5I_8$ of the Ho^{3+} ion splits into two groups of sublevels separated by a gap of the order of 200 cm^{-1} with a total splitting of 500 cm^{-1} (the lower group of sublevels contains 6 electronic states: doublet Γ_3, triplet Γ_5 and singlet Γ_1). In the CF of deformed octahedra with C_s symmetry in Ho1 and Ho2 positions in the SrY_2O_4 crystal, the degeneracy of doublets and triplets is removed, however, as follows from the measured luminescence spectra (Fig. 2 and Table 1), qualitatively the same Stark structure of the ground multiplet is retained, 6 lower singlets are observed in the energy range below 100 cm^{-1}, and the energies of the excited sublevels exceed 300 cm^{-1}, which indicates the dominant role of the cubic component of the CF compared to the rhombic component in both Ho1 and Ho2 positions of holmium impurity ions.

The magnetic moments of quasi-doublets formed by singlets of the same symmetry (Γ_1 or Γ_2) are directed

Table 2. CF parameters (cm^{-1}) in two nonequivalent positions Y1 and Y2 of RE impurity ions in SrY_2O_4

p	k	Ho1	Er1 [16]	Ho2	Er2 [16]
2	0	200.3	188	−8	17
2	2	143.1	137.5	−748	−744
2	−2	−142.6	−171.2	−133	−125
4	0	−59.45	−57.3	−63	−60.2
4	2	−1068.3	−1066.2	1100	1033.2
4	−2	1186.6	1165.2	−981	−977.8
4	4	−62.4	−86.9	408	430.2
4	−4	−942	−972.3	−715	−685.6
6	0	−40.95	−38	−36.9	−35.2
6	2	−22.1	−22.3	−70	−68.4
6	−2	23.1	22.8	−37.4	−42.8
6	4	3.8	30.1	−73	−80.2
6	−4	−151.1	−115.2	−208	−191.4
6	6	−155.7	−162.2	−115	−119.6
6	−6	−99.3	−84	95	80.5

along the **c** axis, but in the case of two closely spaced singlets of different symmetry (Γ_1 and Γ_2), the magnetic moment of the corresponding quasi-doublet lies in the **ab** plane. As follows from the calculations of the spectra using the CF parameters obtained in this paper (Table 2), the ground quasi-doublet contains singlets of Γ_2 symmetry in the Ho1 positions, calculated g-factor of $g_{cc} = 15.65$ agrees well with the one measured ($g_{cc} = 15.71$) in [15]. The ground quasi-doublet in position Ho2 contains singlets of Γ_1 and Γ_2 symmetry, the calculated values of the g factors along the axes **a** and **b** are equal to $g_{aa} = 2.764$ and $g_{bb} = 19.205$. Thus, the principal value of the g-factor is equal to $g_{\perp} = 19.4$, and the corresponding principal direction in the plane **ab** makes an angle $\varphi = 8.2^{\circ}$ with the axis **b**, which agrees with the EPR [15] measurement data ($g_{\perp} = 19.31$, $\varphi = 8.5^{\circ}$).

Let us note that the hyperfine structure of the ground quasi-doublet of Ho2 ions, which is unresolved in the optical spectra and contains 8 electron-nuclear doublets in the energy range $0-2.1\,\mathrm{cm}^{-1}$, substantially broadens the lines of optical transitions involving the ground state of Ho2 ions.

Conclusion

The Stark structure of the $^5I_8$, $^5I_7$, $^5I_6$, $^5S_2$ and $^5F_4$ multiplets of two structurally nonequivalent impurity centers of Ho^{3+} ions in SrY_2O_4 crystal is determined based on studies performed by selective laser spectroscopy. Comparison of the zero-field splittings of the ground quasi-doublets of the $^5I_8$ multiplet, obtained by EPR measurements in the submillimeter range [15] ($\Delta(\mathrm{Ho1}) = 4.303\,\mathrm{cm}^{-1}$, $\Delta(\mathrm{Ho2}) = 1.667\,\mathrm{cm}^{-1}$) and optical spectroscopy (Table 1), allowed us to uniquely identify the measured spectra as spectra of Ho^{3+} ions in positions Y1 and Y2 of the crystal lattice. Calculations performed within the CF theory confirm this conclusion and describe well both the Stark structure of energy levels and the g factors of the ground quasi-doublets of Ho1 and Ho2 ions.

The energies of the three lower sublevels of the ground multiplet of holmium ions obtained in the paper [13] from measurements of the inelastic neutron scattering spectrum in the $SrHo_2O_4$ crystal differ from our results by no more than $2.3\,\mathrm{cm}^{-1}$, which indicates insignificant changes of CF in the positions of the Ho^{3+} ions upon replacement of a significant part of the magnetic ions by diamagnetic ions of yttrium.

The results of this paper open up the opportunity of developing a microscopic theory of the magnetic properties of a magnetically concentrated frustrated quasi-one-dimensional magnet $SrHo_2O_4$ and determining the mechanism for the formation of coexisting ordered and disordered magnetic phases, which were observed at low temperatures in [3,4,9].

Acknowledgments

The authors would like to thank O.A. Petrenko and O. Young for discussing the results of this work.

Funding

This study was supported by grant № 19-12-00244 from the Russian Science Foundation.

Conflict of interest

The authors declare that they have no conflict of interest.

References

[1] Ruby Priya, Sandeep Kaur, Utkarsh Sharma, O.P. Pandey, Sanjay J. Dhoble. J. Mater. Science: Materials in Electronics, **31** (16), 13011 (2020). DOI: 10.1007/s10854-020-03930-6
[2] T.J. Hayes, G. Balakrishnan, P.P. Deen, P. Manuel, L.C. Chapon, O.A. Petrenko. Phys. Rev. B, **84**, 174435 (2011). DOI: 10.1103/PhysRevB.84.174435
[3] O. Young, A.R. Wildes, P. Manuel, B. Ouladdiaf, D.D. Khalyavin, G. Balakrishnan, O.A. Petrenko. Phys. Rev. B, **88**, 024411 (2013). DOI: 10.1103/PhysRevB.88.024411
[4] J.-J. Wen, W. Tian, V.O. Garlea, S.M. Koohpayeh, T.M. McQueen, H.-F. Li, J.-Q. Yan, J.A. Rodriguez-Rivera, D. Vaknin, C.L. Broholm. Phys. Rev. B, **91**, 054424 (2015). DOI: 10.1103/PhysRevB.91.054424
[5] N. Qureshi, A.R. Wildes, C. Ritter, B. Fåk, S.X.M. Riberolles, M. Ciomaga Hatnean, O.A. Petrenko. Phys. Rev. B, **103**, 134433 (2021). DOI: 10.1103/PhysRevB.103.134433
[6] Thomas J. Hayes, Olga Young, Geetha Balakrishnan, Oleg A. Petrenko. J. Phys. Soc. Jpn., **81**, 024708 (2012). DOI: 10.1143/JPSJ.81.024708
[7] T.H. Cheffings, M.R. Lees, G. Balakrishnan, O. A. Petrenko. J. Phys.: Condens. Matter, **25**, 256001 (2013). DOI: 10.1088/0953-8984/25/25/256001
[8] D.L. Quintero-Castro, B. Lake, M. Reehuis, A. Niazi, H. Ryll, A.T.M.N. Islam, T. Fennell, S.A.J. Kimber, B. Klemke, J. Ollivier, V. Garcia Sakai, P.P. Deen, H. Mutka. Phys. Rev. B, **86**, 064203 (2012). DOI: 10.1103/PhysRevB.86.064203
[9] Olga Young, Geetha Balakrishnan, Pascal Manuel, Dmitry D. Khalyavin, Andrew R. Wildes 3, Oleg A. Petrenko. Crystals, **9**, 488 (2019). DOI: 10.3390/cryst9100488
[10] O.A. Petrenko, O. Young, D. Brunt, G. Balakrishnan, P. Manuel, D.D. Khalyavin, C. Ritter. Phys. Rev. B, **95**, 104442 (2017). DOI: 10.1103/PhysRevB.95.104442.
[11] N. Qureshi, O. Fabelo, P. Manuel, D.D. Khalyavin, E. Lhotel, S.X.M. Riberolles, G. Balakrishnan, O.A. Petrenko. SciPost Physics, 11, 007 (2021). DOI: 10.21468/SciPostPhys.11.1.007
[12] H. Karunadasa, Q. Huang, B.G. Ueland, J.W. Lynn, P. Schiffer, K.A. Regan, R.J. Cava. Phys. Rev. B, **71**, 144414 (2005). DOI: 10.1103/PhysRevB.71.144414
[13] S. Ghosh, H.D. Zhou, L. Balicas, S. Hill, J.S. Gardner, Y. Qiu, C.R. Wiebe. J. Phys.: Condens. Matter., **23**, 164203 (2011). DOI: 10.1088/0953-8984/23/16/164203
[14] A. Fennell, V.Y. Pomjakushin, A. Uldry, B. Delley, B. Prevost, A. Desilets-Benoit, A.D. Bianchi, R.I. Bewley, B.R. Hansen, T. Klimczuk, R.J. Cava, M. Kenzelmann. Phys. Rev. B, **89**, 224511 (2014). DOI: 10.1103/PhysRevB.89.224511

[15] G.S. Shakurov, B.Z. Malkin, R.G. Batulin, A.G. Kiyamov. Opt. i spektr., **130** (1), 28 (2022) (in Russian). DOI: 10.21883/OS.2022.01.51886.24-21
[16] B.Z. Malkin, S.I. Nikitin, I.E. Mumdzhi, D.G. Zverev, R.V. Yusupov, I.F. Gilmutdinov, R. Batulin, B.F. Gabbasov, A.G. Kiiamov, D.T. Adroja, O. Young, O A. Petrenko. Phys. Rev. B, **92**, 094415 (2015). DOI: 10.1103/PhysRevB.92.094415
[17] W.T. Carnall, G.L. Goodman, K. Rajnak, R.S. Rana. J. Chem. Phys., **90**, 3443 (1989). DOI: 10.1063/1.455853
[18] M. Mazzera, R. Capelletti, A. Baraldi, N. Magnani, M. Bettinelli. J. Phys.: Condens. Matter., **24**, 205501 (2012). DOI: 10.1088/0953-8984/24/20/205501
[19] V.V. Klekovkina, A.R. Zakirov, B.Z. Malkin, L.A. Kasatkina. J. Phys.: Conf. Ser., **324**, 012036 (2011). DOI: 10.1088/1742-6596/324/1/012036
[20] B.Z. Malkin. In: *Spectroscopy of Solids Contaning Rare Earth Ions,* ed. by A.A. Kaplyanskii, R.M. Macfarlane (North-Holland, Amsterdam, 1987), ch. 2, 13–50.
[21] A. Abragam, B. Bleaney. *Electron Paramagnetic Resonance of Transition Ions* (Oxford Univ. Press, Oxford, 1970).
[22] M.A.H. McCausland, I.S. Mackenzie. Adv. Phys., **28**, 305 (1979). DOI: 10.1080/00018737900101385

Translated by E.Potapova